Particle Accelerators
1979, Vol. 9, pp. 169–186

ION ACCELERATION BY SUPERCONDUCTING RESONATORS

ILAN BEN-ZVI

Department of Physics and High Energy Physics Laboratory, Stanford University, Stanford, California U.S.A.†

and

Department of Nuclear Physics, The Weizmann Institute of Science, Rehovot, Israel‡

(*Received August 4, 1977*)

The application of rf superconductivity techniques to ion acceleration is discussed. Resonator properties are evaluated, with emphasis on the reentrant cavity, $\lambda/2$ helix and split-ring resonators. The properties of a short linac section for boosting the beam energy of tandem Van de Graaffs are discussed, including beam dynamics, cryogenics, and electronics. A detailed description of the techniques for the construction and processing of niobium reentrant cavities is given.

1 INTRODUCTION

RF superconducting techniques are particularly well suited to the design requirements of an accelerator for producing a high quality beam of ions in the intermediate and heavy mass region. The advantages of the superconducting techniques are several-fold. First, superconducting structures can be operated continuously (with 100% duty factor), drawing a negligible total amount of power, orders of magnitude lower than the best room-temperature structure. Second, the mode of operating the accelerator can be extremely flexible. Due to the small rf power dissipation in superconducting structures, it is practical to design an accelerator as a sequence of independent cavities which are independently driven using low-power solid-state rf devices. This arrangement provides low cost independent phase and amplitude control for each cavity and thereby enables one to program the velocity profile along the accelerator as desired. The result is a capability of varying the beam energy and great flexibility in accelerating ions of different charge-to-mass ratio. Third, a superconducting accelerator can produce beams of high quality. The possibility of stabilizing the accelerating fields in each cavity both with respect to amplitude and phase leads directly to the possibility of generating beams with good energy resolution and good transverse phase space.

The physics interest in producing high quality beams of ions in the intermediate and heavy mass region at increasing energy is large. There is a rather large practically unexplored region of experimental nuclear physics, which requires light to intermediate weight ions, with good beam quality such as a Van de Graaff gives, but with higher energy than present Van de Graaffs can achieve. The special features which lend significance to heavy ions are their large electric charges, their large masses and the large linear and angular momenta that they can transfer to target nuclei in a nuclear reaction. High electric charge is important for Coulomb excitation and the study of static quadrupole moments, transition E4 and E6 moments and the excitation of states of very high angular momentum. The large mass, as well as particular charge-to-mass ratios, make it possible to produce a variety of esoteric nuclei, in particular neutron poor nuclei, which cannot be produced in any other way. The large angular momentum transferred in some heavy ion reaction leads to nuclear excitation in high Yrast states. These are of interest in their own right, but they also lead, after a sequence of decays, to the production of low-lying nuclear levels with high angular momenta, objects of considerable interest in nuclear physics today. Large linear momentum transfer leads to high recoil velocities and these are of significance in two areas involving electromagnetic properties of nuclei. One is the plunger-type measurement of nuclear lifetimes and

† Work supported in part by grants from the U.S. National Science Foundation Grant 33411.

‡ Work supported in part by the U.S.-Israel Binational Science Foundation under Grant 926.

the other, the hyperfine interaction of nuclei in isolated ions. In both areas the range and significance of the measurement increases considerably with increased recoil velocity. The ideal reaction for such purposes is ordinary light ion reactions like (d, p) or (p, α), with the usual roles of target and projectile interchanged. Such reactions therefore call for a large variety of projectiles and also, because of the need for particle-gamma coincidence detection, high-beam quality and high-duty cycle.

The success of electrostatic accelerators, as evidenced by the number of machines built and the scope of research that has been done on them should serve as a guide to the properties of the next generation of accelerators. These properties are: a) good energy resolution, b) unity duty cycle, c) small transverse beam spread, and d) flexibility. The last means that we can change the ion species and energy very easily, and that useful energies are obtained for many different ions.

The beam current of ions, while not very impressive (usually being under 1 μA), is adequate for most of the work.

The limitations of electrostatic accelerators are the energy and the mass of the particles with sufficient energy per nucleon. As methods and ideas are developed and more interesting problems come into focus, one is almost always led to requirements on the particle beams which are beyond the capabilities of any electrostatic machine. The solution to this problem would be a machine which relatively small laboratories could afford, which would have the mentioned properties of a tandem but would extend the energy and mass number. It is true that a number of accelerators, or rather acceleration combinations such as tandem cyclotrons have been proposed which can achieve the beam properties mentioned. While one could not call these machines "conventional," since the problems encountered in any of the approaches are far from being conventional, they are based on accelerator technologies which have matured in other applications, and certainly could be built and operated successfully. The problem of such machines is the cost, which is far beyond the means of the average laboratory, and even for large national laboratories most of these proposals have been rejected. What is called for is a "poor man's accelerator," which will cost no more than a modern tandem, and will have the same beam quality, but extend the energy range of a tandem.

The fact that so many nuclear physics laboratories have tandem accelerators suggests the development of a booster accelerator, which will accept the tandem output, and will increase the energy without imparing resolution, duty cycle, and beam spread. Furthermore, such a booster should come in various sizes as the needs and means call for, and space allowing, be extendable for future expansion. The superconducting linac is such a solution, and is the subject of this article.

The next chapter contains a discussion on resonator properties and design considerations, comparing a few resonators in respect to their performance as superconducting-ion accelerating units.

Chapter 3 deals with the structure and characteristics of a booster linac made with the resonators of Chapter 2. It includes a description of the accelerator structure, beam dynamics, cryogenic, and electronic properties.

Chapter 4 is devoted to the techniques involved in manufacturing that important building stone of the cryogenic linac—the superconducting resonator. Since there are different procedures for the various resonators, the discussion centers on the reentrant cavity, but the techniques described are suitable for other superconducting resonators as well.

2 RESONATOR DESIGN

The most basic and important unit of a linear accelerator is the resonator. Many superconducting resonators have been built and tested. The most popular resonators for heavy ion acceleration are the reentrant cavity,[1,2] the helix[3,4] and the split ring.[5,6] The function of the resonator in a linac is to generate a high accelerating field at a lower power consumption. The quantity that measures its performance in this respect is the shunt resistance, Rs. However, the power consumption of superconducting structures is small so that other properties besides Rs become as significant, such as stability, simplicity in construction and maintenance, cooling capacity and many others.

The following subsections treat significant properties of resonators for heavy-ion cryogenic accelerators.

2.1 *Material Properties*

To date the best results have been obtained with niobium resonators. Type I materials, the best of

which is lead, are inferior both in surface resistance and the critical magnetic field.

The surface resistance R is related to the power lost per unit area p by the relation

$$p = \frac{RH_0^2}{2} \quad \text{(mks)},$$

where H_0 is the peak applied surface rf magnetic field of a sinusoidally time-varying field.

The surface resistance of superconducting resonators R has been experimentally determined to be given by:[7]

$$R(T) = R_r + R_{sc}(T),$$

where the residual resistance R_r is the temperature-independent part and is believed to be due to surface contamination, since its value varies from resonator to resonator. The superconducting resistance $R_{sc}(T)$ follows a theoretically predictable curve[8] and for niobium is given by[9]

$$R_{sc}(T) = R_0 f^{1.80} \exp\left(-\frac{15.2}{T}\right),$$

where $R_0 = 12.4\ \mu\Omega$, the rf frequency f is in GHz, and the temperature T is in kelvins.

The residual resistance in well prepared niobium resonators is of the order of $10^{-9}\ \Omega$. Depending on the operating frequency, $R_{sc}(T)$ becomes comparable to R_r between 2°K and 4°K. Besides the surface resistance, another important material property is the limiting field level. Since it was discovered that in type II superconductors one can operate resonators with $H_0 > H_{C1}$,[10] work has been started on Nb_3Sn,[11] $M_0 - R_e$,[12] etc., and some of the results seem promising. However, niobium technology is still better developed, so this report will be confined to niobium resonators. The material limitations on the field level come from electron-field emission or multipactoring, and thermal runaway which starts at a certain "break down" field level.

The quality of the surface is detrimental for the attainment of high surface electric and magnetic fields. The maximum surface electric field that can be achieved in a resonator, E_m, depends on the surface microstructure, on adsorbed gasses,[13] and on the ever-present oxide layer.[14] If the surface is not clean enough, even low-field multipactoring levels cannot be passed through. Clean surfaces with adequate cooling are limited at peak surface electric fields of about $E_m \sim 15$–25 MV/m for the low-frequency structures used in heavy-ion work, although considerably higher surface fields were attained at x band.[10] This limitation starts as field emission, manifesting itself by power dissipation and x-ray emission from the stopped electrons. As the field is pushed higher, the heating of the resonator may cause a thermal runaway, usually called "breakdown," because it happens on a very short time scale, typically a few microseconds. In regions where the surface electric field is low but the surface magnetic field is high, the field in the cavity can be limited by a maximum magnetic field H_m. This limit can appear as a "slow breakdown" (time scale of milliseconds) due to the heating of a relatively large surface area (about 1 cm^2) caused by poor thermal conduction to the liquid helium bath, or as a "fast breakdown" (time scale of microseconds) caused by a small "bad spot" going normal. Such a bad spot on the surface can be caused by impurities concentration, and once the dimensions of the normal conducting area reach $\sim 1\ \mu$, it can grow at a rate of 10^8 m/sec.

A well-constructed and cleaned superconducting resonator can be expected to reach H_m over 0.1 tesla. This field level is high enough to make E_m the upper limit on the resonator field. The properties of niobium surfaces for rf superconductivity work are given by Halbritter.[15]

The niobium for resonator manufacturing can be purchased from a number of producers, e.g., Wah Chang Albany Corp., Fansteel and Kawecki-Berylco Corp. The impurity content given in Table I[16] should be requested. This specification is known as "Stanford quality" niobium, and can be obtained without any large price increase over the standard "reactor grade." In addition to the impurity limits, the niobium should be free of voids and inclusions, and annealed. The manufacturing and treatment of the resonators is discussed in section 4.

TABLE I

Maximum impurity limits for Nb in part per million

Al 20	H 10	Pb 20
B 2	Hf 100	Si 50
C 30	Mg 20	Sn 20
Ca 20	Mn 20	Ta 300
Cd 5	Mo 50	Ti 40
Co 20	N 60	V 20
Cr 20	Ni 20	W 100
Cu 40	O 150	Zr 100
Fe 50		

2.2 *Mechanical and Cryogenic Properties*

Without going into the details of the particular resonator design, we note that there are some important dimensions and features which affect its performance as an accelerating structure.

a) The gap g is the size of the region where a unidirectional accelerating electric field E_a appears. There may be more than one gap in the resonator (e.g., two in the spiral, three in the split ring), and the field E_a need not be constant in space over the gap (e.g., the helix).

b) The total length of the resonator l is the center-to-center distance between two successive resonators in an accelerating structure. The ratio g/l should be as large as possible, to utilize efficiently the available space.

c) The beam tube diameter d is the clear bore available for the beam. Its minimum size is dictated by beam-dynamics calculations. In boosting the energetic beam of a tandem, a couple of centimeters is enough.

d) The total resonator diameter D is not very critical, however, it should be small enough for convenient machining, a reasonable cryostat size and for the saving of structural material, niobium.

e) Good mechanical stability is particularly important for superconducting structures where ponderomotive oscillations and static instabilities can be quite troublesome. The minimum threshold energies for ponderomotive oscillations and for static instabilities are both inversely proportional to the quantity $K_0 \equiv (1/U)(\Delta f/f)$, where U is the stored electromagnetic energy in the resonator, Δf is the radiation pressure induced frequency shift at a stored energy U, and f is the resonance frequency.

f) The frequency of the lowest mechanical resonance, F_0, should be as high as possible, since this resonance introduces a pole in the frequency control circuit of the resonator for mechanical tuning, and a peak in the phase noise spectrum.

g) A simple geometric shape is decisive in the constructional cost of the resonator. Because there is no quantity that measures this quality, it is often overlooked in comparative studies.

h) The cooling capacity of the resonator determines the maximum field limit of thermal runaway. To provide good cooling, the wall thickness should be small and the material degassed to improve the thermal conductivity. For resonators operating in superfluid helium, the exterior of the cavity should be chemically polished to reduce the Kapitza resistance[17] which may become the limitation on the heat transfer from the resonator to the helium.

In some resonators (e.g., the helix, the split ring) most of the power is dissipated on a thin tube of niobium, which is cooled by helium flowing inside the tube. In this case the limit on the heat conductance is the circulation of the helium. For high-power operation care must be taken to improve the circulation, like operation with superfluid helium or with a forced circulation.

Three types of resonators which are popular in heavy-ion superconducting work are the reentrant cavity, shown in Figure 1, the helix in Figure 2, and the split ring in Figure 3.

The dimensions of these resonators are given in Table II. The resonators shown in Table II are the 430 MHz reentrant cavity of the Stanford–Weizmann Institute collaboration,[1] the $\lambda/2$ helix of Karlsruhe Nuclear Research Center which was built for the Max–Planck-Institute,[4] and Argonne National Laboratory's split ring.[6] Another split ring

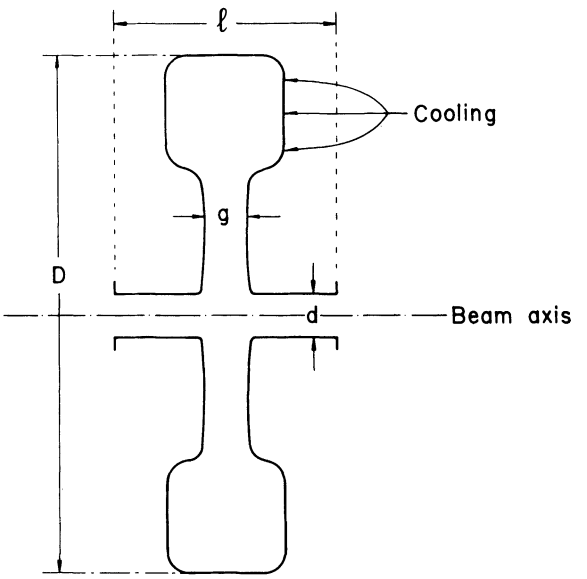

FIGURE 1 A reentrant cavity.

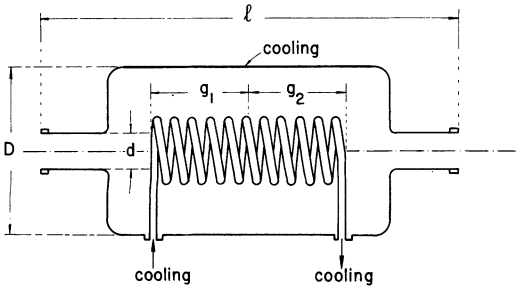

FIGURE 2 A helix resonator

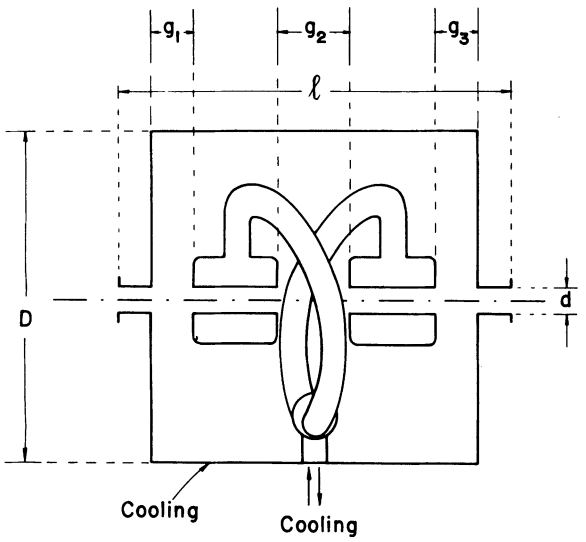

FIGURE 3 A split ring resonator.

is being developed by a Stony Brook–Cal Tech collaboration.[18] The gap size entry, (g), gives the length along the beam axis of the unidirectional accelerating field region, not including fringing field penetration into the beam tubes.

The length of the resonator does not include the beam-tube connections which are included in the next entry (l). Since l was not available for the split ring, the calculation of electrical properties in the next subsection was done with the resonator length. The beam tube diameter (d) and total diameter (D), as well as gap size for the split ring are approximate figures.

The static frequency shift constant $(1/Ea^2)(\Delta f/f)$ was given in terms of the accelerating field rather than the stored energy for convenience. The figure for the reentrant cavity is for a basic cavity, without struts. Strutting should improve this figure by an order of magnitude. The helix cannot be supported,

TABLE II

Mechanical properties of typical resonators

Mechanical property	Reentrant cavity	$\lambda/2$ helix	Split ring
g (cm)	2	8.25, 8.25	3.8, 7.6, 3.8
Resonator length (cm)	8	24	35.5
l (cm)	10	29.5	—
d (cm)	2	5	3.8
D (cm)	38	16	41
$\frac{1}{E_a^2}\frac{\Delta f}{f}$ (MV/m)$^{-2}$	1.2×10^{-6}	5.2×10^{-5}	1.6×10^{-6}

and in the split ring only the cylindrical housing can be strutted. The strutted reentrant cavity is therefore the most stable structure.

The high stability reflected by the significantly small values of $(1/Ea^2)(\Delta f/f)$, considerably simplifies the cost and complexity of the electronics and eliminates an appreciable refrigeration loss which is created by the high power rf lines which are necessary to provide frequency control in helices.

The complexity of a resonator construction is something which is not easily measured. Since the major component in the cost of a resonator is labor, the split ring is quite expensive as some 70 separate welds are made in its construction. The reentrant cavity has a high degree of symmetry and can be manufactured by hydroforming plates of niobium, and machined on a lathe. The cavity and probes need about 6 electron beam welds, and the struts another 12 TIG welds. The helix construction is intermediate in complexity. However, one split-ring resonator can do the job of a number of reentrant cavities in terms of acceleration voltage (see Table III), and this advantage offsets its relative high cost.

TABLE III

Electric properties of typical resonators

Quantity (see text)	Units	Reentrant cavity	$\lambda/2$ helix	Split ring
f	MHz	430	108	97
Γ	ohm	67	7	16
R_s^*	ohm^2/m	4.6×10^4	8.1×10^4	8.7×10^4
N	—	3.1	3.3	0.85
E_p	MV/m	4.0	12.8	4.8
H_p	Gauss	60	500	176
U	Joule	0.05	0.10	0.17
β_{opt}	—	≥ 0.1	0.10	0.115

2.3 *Electric Properties*

The significance of any electric property of a resonator depends on the intended use. The particular use as a superconducting accelerating structure for heavy ions is quite different from that of room-temperature use. The resonator parameters which have been selected for comparison in Table III are those which, in the author's opinion, best reflect the usefulness of these resonators as superconducting heavy-ion accelerators.

The frequency enters into the expression for the superconducting surface resistance (Section 2.1.), the transit time factor and the beam dynamics (Section 3.2.). The transit time factor is a function of the product of the gap and the frequency, therefore the gap length is limited by the operating frequency for a given particle velocity. This is the reason for the short length of the reentrant cavity, and that is why it takes about four reentrant cavities to give the same voltage gain of one split ring. This property is expressed by the entry N which is defined as: N = the number of resonators needed for an energy gain of one MeV per charge, for particles at the velocity β_{opt}, and resonators operated at the peak surface electric field of 15 MV/m, and phase 0°.

The choice of the peak-surface electric field as the limit on the resonator performance is made in view of the experimental results.

The geometric factor Γ is a surface resistance independent measure of the quality factor, $\Gamma = QR$. It is not important in a direct way but it is necessary information in order to calculate resonator properties, such as derivation of the shunt resistance Rs from the ratio of accelerating field squared to the stored energy. In the case of the helix, the geometric factor was derived from Figure 6 of Ref. 19, using the geometry of Table II.

The quantity R_s^* of Table III is the shunt resistance per unit length multiplied by the surface resistance, $R_s^* = R_s R/l$. This quantity is surface-resistance independent and is useful in comparing the power per unit length at a given gradient.

The quantities E_p and H_p are significant for superconducting resonators. They represent the peak surface electric field and peak surface magnetic field anywhere in the resonator, normalized to an accelerating electric field of 1 MV/m.

Since the peak surface field, electric or magnetic, will limit the accelerating field of the structure, the smaller these figures are the higher the voltage gradient. For the time being the electric field is the limit. However, as processing techniques improve, the peak-surface electric field for regular operation gets larger, and then the critical magnetic field of niobium may limit the resonator through H_p.

Finally, β_{opt} is the designed particle velocity/c of the resonator. For the multiple-gap resonators this is the velocity at which the transit time factor is maximal.

3 ACCELERATOR PROPERTIES

On the basis of typical performance of superconducting cavities it is possible to design an accelerator for $\beta \sim 0.1$ particles which operates with a 100% duty factor at a voltage gradient of 2–3 MV/m. The rf dissipation in the superconducting structure is expected to be less than 10 W/m. Therefore it is possible to find room for a short linac section in most tandem laboratories without excessive rebuilding and relocation of major equipment. The modest liquid helium consumption is compatible with an average laboratory helium liquefier. To preserve the convenient features of a tandem such as simple selection of the ion's charge-to-mass ratio and energy variability, the accelerating structure has to be made of individually phased single resonators.

3.1 *The Accelerator Structure*

Figure 4 shows a tentative tandem-cryogenic booster set-up. The tandem beam, following a 90° magnet, is chopped and bunched by superconducting cavities in the first dewar. The bunched beam is then accelerated through N dewars, each containing n cavities (in Figure 4 $N = 9$, $n = 10$). Between dewars we have radial focusing lenses. The lenses could be superconducting solenoids and inserted inside the cryostats. In this case one could have more than one structure per cryostat. The last component is a debuncher cavity, preceded by a suitable drift length, whose function is to remove most of the energy modulation imparted to the beam by the buncher.

Pressure transparency is no problem here. Since the booster operates at liquid helium temperature, the only gas source could be a helium leak. Once helium leaks have been eliminated, the accelerator does not require pumping, and a small helium leak can be tolerated by using turbomolecular pumps between dewars. On the other hand, since the accelerating structure is in fact a powerful cryopump, good isolation between the injector (the

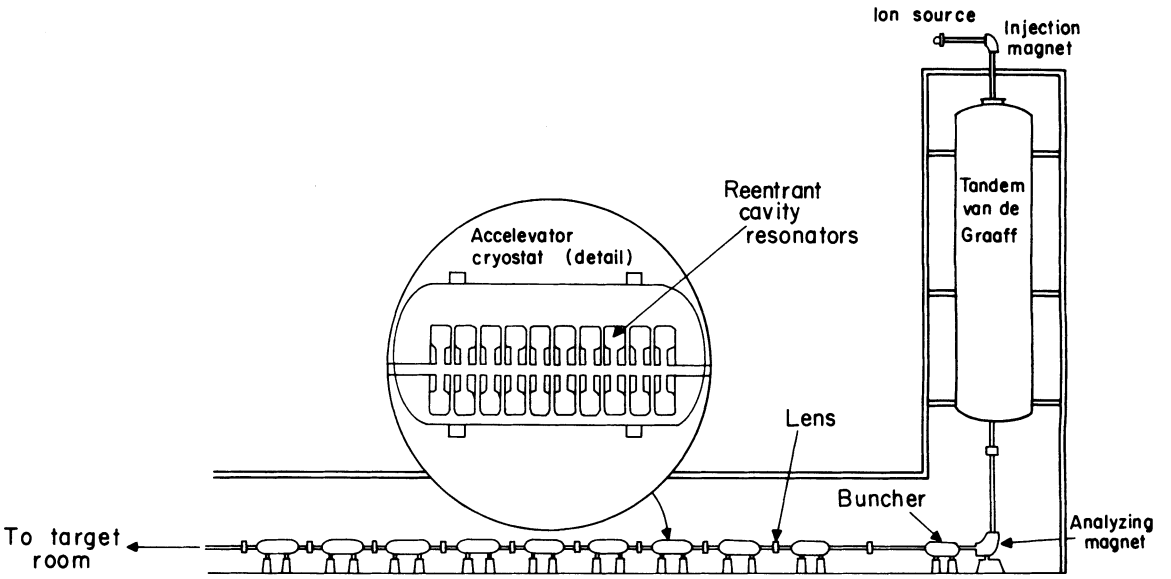

FIGURE 4 A tandem-cryogenic booster accelerator.

tandem), the target room and the booster is necessary to prevent contamination of superconducting structures. A reasonable amount of differential pumping at each end will provide sufficient isolation.[20]

The power consumed by the accelerating structure and the length needed depends on the resonator type. Let us assume a surface resistance of 10^{-8} ohms and 15 MV/m peak surface electric field as the resonator's material performance. Suppose now that we require 10 MV total voltage drop across the linac (not including transit time factor, and at a stable phase of 0°) and ask how much rf power is dissipated in the liquid helium, and how long the structure is (not including unavoidable dead spaces such as focusing lens, interconnections, etc.). The answer is summarized in Table IV. Actually, this is just another representation of the resonator properties given in Tables II and III, but one which is significant for accelerator construction purposes.

TABLE IV

Accelerating structure for a 10 MV linac

	Reentrant cavity	$\lambda/2$ helix	Split ring
Total rf power, watts	8.2	1.5	3.6
Structure length, meters	2.7	8.5	3.2
Watt/meter	3.0	0.17	1.1

The rf power figures are related to the resonators only. Static loss of the cryostat, to which a major contribution comes from electric connections, can be considerably larger than the resonator losses given in Table IV. For example, test of helix cryostats in Karlsruhe shows static loss rates of 4 to 5 watts/meter,[21,4] and tests of an experimental reentrant cavity cryostat at Stanford[22] shows losses of about 2 watts/meter. Therefore, unless the performance of cryostats improves markedly, there is no point in improving the resonator shunt resistance at the expense of other parameters.

3.2 *Beam Dynamics*

Some of the material of this section has been discussed in greater detail in a previous communication.[23]

Before the beam is accelerated by the linac structure it has to be matched to it in longitudinal phase space (energy and phase) and transverse phase space (radial position and momentum). The matching is done with a chopper-buncher and lens, respectively. Results of numerical beam-dynamics calculations,[24] as well as experimental results,[25] show that it is possible to have the dc beam of a tandem chopped and bunched to pulses short enough even for a 400 MHz linac, with a good transmission (about 15%).

The beam is matched to the accelerator if it satisfies the two following conditions:

$$\frac{\Delta W_m}{\psi_m} = \left(- \frac{qeE_a \sin \phi_s \beta^3 \gamma^3 m_0 c^2}{k} \right)^{1/2} \tag{3.2.1}$$

$$\frac{r'_m}{r_m} = \nu_r \tag{3.2.2}$$

ΔW_m and ψ_m are the energy and phase semi axes of the beam ellipse in longitudinal phase space (measured relative to the standard particle), and r_m, r'_m are the radial position and angle ellipse semi axes. Also:

q = ion charge/e,
e = electron charge
E_a = traveling wave gradient (including the transit factor),
ϕ_s = stable phase ($\phi_s < 0$)
$\gamma = (1 - \beta^2)^{-1/2}$,
$m_0 c^2$ = ion's rest energy
$k = 2\pi/\lambda$,
for ν_r see Eq. (3.2.13).

The operating conditions of booster linacs (post accelerators) of tandem Van de Graaffs are unusual, since the emittance of the tandem is very small. Thus there is no need to worry about the linac acceptance. On the other hand, one worries about the beam quality, since most nuclear physics experiments need small beam emittances in both phase spaces. The longitudinal emittance, $e_\psi = \pi \Delta W_m \psi_m$, and the transverse emittance, $e_r = \pi r_m r'_m$, can be degraded by a few side effects of the accelerating process. Some of these effects are nonlinearity of the bunching process in the accelerator, interactions between the longitudinal and transverse phase spaces, and more.

Operating near the $\pi/2$ mode and with ψ_m small compared to ϕ_s, the nonlinearity effect can be written approximately as

$$\frac{\delta e_\psi}{e_\psi} \lesssim \frac{1}{4} \Omega ctg \Omega \psi_m ctg \phi_s \tag{3.2.3}$$

where δe_ψ is the apparent increase in e_ψ, and Ω is the rotation angle of the phase space ellipse in one section of the accelerator.

$$\Omega = \int_{\text{section}} k_\psi \, dz \tag{3.2.4}$$

$$k_\psi = \left(\frac{-kqeE_a \sin \phi_s}{\beta^3 \gamma^3 m_0 c^2} \right)^{1/2} \tag{3.2.5}$$

Ω is nearly equal to the mode μ, and since we prefer $\Omega \approx \pi/2$ [just by looking at (3.2.3)] the mode μ is given by

$$\cos \mu = \cos \Omega - \tfrac{1}{2} k_\psi D \sin \Omega \approx - \tfrac{1}{2} k_\psi D. \tag{3.2.6}$$

D is the drift length between sections.

The Bessel-function dependence of the accelerating field on the radial coordinate r produces two deterioration effects in the longitudinal phase space. The first is similar in form (3.2.3) and can be written as

$$\frac{\delta e_\psi}{e_\psi} \lesssim \tfrac{1}{8} (k_r R)^2 \Omega \operatorname{ctg} \Omega, \tag{3.2.7}$$

where

$$k_r = \frac{k}{\beta}, \tag{3.2.8}$$

and we can see that $\Omega = \pi/2$ cancels this effect too.

The second effect produces a steady increase in the phase-space area, which is proportional to the length of the accelerator squared. This effect places the most stringent limitation on the radial acceptance. Particles which, on the average, stay off axis gain steadily more energy than other particles which stay near the resonator axis. The increase in the phase excursion is approximately

$$\Delta \psi(r) \approx \tfrac{1}{8} (k_r r)^2 (k_\psi Z)^2 \operatorname{ctg} \phi_s. \tag{3.2.9}$$

Equation (3.2.9) can be written as a limit on the accelerator's length, Z, or the average radial excursion in the accelerating structure

$$(\overline{r^2})^{1/2} \lesssim \sqrt{\frac{8 \Delta \psi_m}{\operatorname{ctg} \phi_s}} \frac{1}{K_r k_\psi Z^2}, \tag{3.2.10}$$

where $\Delta \psi_m$ is an upper limit on the phase excursion.

The transfer matrix for the radial variables r and $r' = dr/dZ$ from the center of one lens to the center of the next lens (thus including a lens of half power, $1/2F$, one half of the drift length $D/2$, an acceleration section, half a drift and a half power lens) is

$$\begin{pmatrix} \cos \mu_r & \frac{1}{\nu_r} \sin \mu_r \\ -\nu_r \sin \mu_r & \cos \mu_r \end{pmatrix} \tag{3.2.11}$$

$$\cos \mu_r = \cos h \frac{\Omega}{\sqrt{2}} + \frac{Dk\psi}{2\sqrt{2}} \sin h \frac{\Omega}{\sqrt{2}} - \frac{1}{2F} \left[\frac{\sqrt{2}}{k_\psi} \left(1 + \left(\frac{Dk_\psi}{2\sqrt{2}} \right)^2 \right) \sin h \frac{\Omega}{\sqrt{2}} + D \cos h \frac{\Omega}{\sqrt{2}} \right] \tag{3.2.12}$$

$$v_r^2 = \frac{\frac{1}{2F}\left(2\cos h\frac{\Omega}{\sqrt{2}} + \frac{k_\psi D}{\sqrt{2}}\sin h\frac{\Omega}{\sqrt{2}}\right) - \frac{k_\psi}{\sqrt{2}}\sin h\frac{\Omega}{\sqrt{2}}}{\frac{\sqrt{2}}{k_\psi}\left(1 + \left(\frac{Dk_\psi}{2\sqrt{2}}\right)^2\right)\sin h\frac{\Omega}{\sqrt{2}} + D\cos h\frac{\Omega}{\sqrt{2}}} - \frac{1}{4F^2} \quad (3.2.13)$$

The matching condition (3.2.2) gives a relation between the radial emittance e_r and the maximal radial excursion

$$e_r = \pi r_m^2 v_r. \quad (3.2.14)$$

To minimize r_m for a given e_r, we have to maximize v_r. Since F is the only free parameter left, we find:

$$F_{\text{opt}} = \frac{1}{2}\cdot\frac{\frac{\sqrt{2}}{k_\psi}\left(1 + \left(\frac{Dk_\psi}{2\sqrt{2}}\right)^2\right)\sin h\frac{\Omega}{\sqrt{2}} + D\cos h\frac{\Omega}{\sqrt{2}}}{\cos h\frac{\Omega}{\sqrt{2}} + \frac{k_\psi D}{2\sqrt{2}}\sin h\frac{\Omega}{\sqrt{2}}} \quad (3.2.15)$$

and

$$v_{r,\text{opt}} = \frac{1}{D\cos h\frac{\Omega}{\sqrt{2}} + \frac{\sqrt{2}}{k_\psi}\left(1 + \left(\frac{k_\psi D}{2\sqrt{2}}\right)^2\right)\sin h\frac{\Omega}{\sqrt{2}}} \quad (3.2.16)$$

The mode which corresponds to this optimum is the $\pi/2$ mode, as can be verified by substituting (3.2.15) into (3.2.12).

3.3 *Cryogenics*

One of the more obvious complications that a superconducting accelerator has is a cryogenic refrigeration system. The main components of this system are the refrigerator and the cryostats. However, both components are available commercially, are dependable and reasonably priced.

A drawing of an accelerator cryostat[26] is given in Figure 5. Details of the cryostat performance will be given in a future communication.[27] The cryostat features a low-static thermal loss, stainless-steel construction and a helium vapor-cooled radiation shield. The large diameter (63 cm) seal of the liquid helium vessel is based on the elasto-plastic principle, with indium metal as the plastic member and a stainless-steel spring as the elastic member. This seal is extremely dependable and can withstand thermal shocks and large thermal gradients, so that fast cool-down and warm-up are possible without breaking the vacuum seal.

The performance of the cryostat is dependent on the electric connections to the resonators. The radiation load can be as low as 0.02 watts/meter (using either helium vapor or liquid nitrogen cooled radiation shield). The figures, quoted in section 3.1. of 2 to 5 watts/meter are for ion-accelerator cryostats, which have numerous electric connections. The heat leak into Stanford's Superconducting Electron Accelerator cryostats is about 0.16 watt/meter,[28] and the variable coupling probe of this electron linac has a measured heat load less than 1 watt at 10 kilowatt incident rf power.[29] Therefore it seems that with some careful cryogenic design the performance of heavy ion linac cryostats should improve to better than 1 watt/meter.

To study the effect of helium bath temperature, let us first assume that we have a linac made of 90 reentrant cavities, which are operated at a peak surface electric field $E_s = 12$ MV/m. Such a linac gives over 21 MV, or about 11-MeV energy gain per charge with $\cos\phi_s$ and the transit time factor included ($\phi_s = 30°$, $\beta = 0.1$).

The heat load, P_d (power dissipated) is given by

$$P_d = \frac{Nl}{R_s^*}\left(\frac{E_s}{E_p}\right)^2 R,$$

with $E_s = 12 \times 10^6$ volt/meter, $N = 90$ and l, R_s^*, E_p taken from Tables II and III, we get

$$P_d = \left(\frac{1.5w}{n\Omega}\right) \times R.$$

The equations for R of section 2.1. can be substituted into this equation to yield P_d versus temperature. Figure 6 shows the results for residual resistances R_r of $2n\Omega$ and $25n\Omega$. The $2n\Omega$ value represents some sort of lower limit on R_r which has been attained by a number of experimentalists over a wide range of frequencies. The $25n\Omega$ value can be considered an upper limit for a reasonably good cavity. Thus the two curves set realistic limits on the refrigeration requirements of this booster.

The operating temperatures of the acceleration cavities can have a pronounced effect on the size and cost of the refrigeration system required to

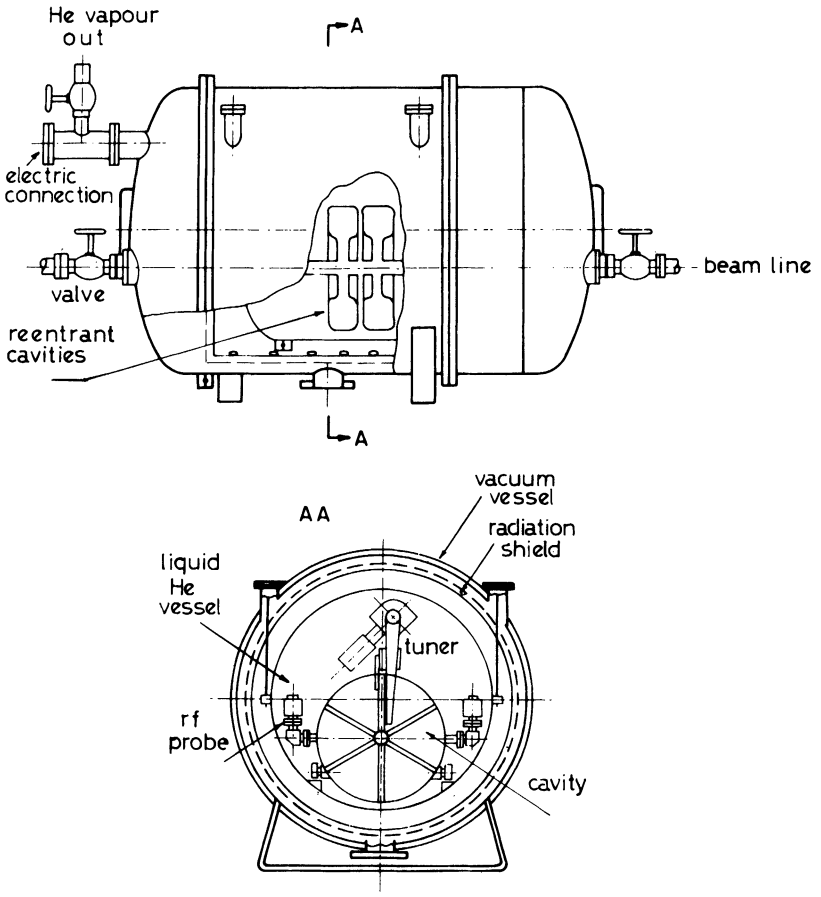

FIGURE 5 A cryostat for superconducting cavities.

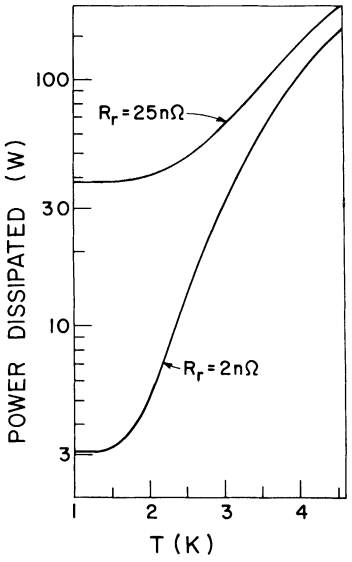

FIGURE 6 Linac power dissipation vs. temperature.

cool them. As Figure 6 demonstrates, lowering of the bath temperature from 4K to 2K can drastically reduce the heat load on the refrigeration system. At the same time, requiring such a temperature decrease necessarily increases the complexity and cost of the refrigeration system per watt of cooling. In order to determine the most economical operating temperature, the cost to cool the 90 cavity booster operating at $E_p = 12$ MV/m is plotted versus temperature in Figure 7. The equations for refrigerator cost were taken from Ref. 30 after correcting for inflation and the difficulty of reaching temperatures below 2K. They represent some sort of averaged costs of actual refrigeration systems. Even though the cost of commercial refrigeration may vary by 50% from the curves, and these refrigerators do not come in a continuum of sizes and prices as the curve might suggest, the curves are useful for indicating general trends of cost.

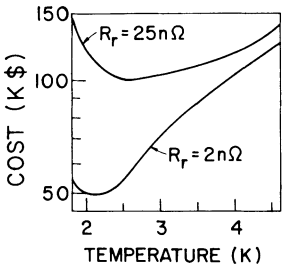

FIGURE 7 The cost of the refrigeration system vs. temperature, for a 90-cavity booster.

An important consideration in the selection of the operating temperature could be the geometry of the resonator for cooling.

A single split ring, operating in the conditions of Table IV, requires about 0.4 watts of refrigeration and a single reentrant cavity under the same conditions, about 0.3 watts. However, the 0.4 watts of the split ring have to be supplied through a tube about 2.8 cm in diameter, or a power density of 6.5×10^{-2} watts/cm^2. The reentrant cavity has about 2.5×10^3 cm^2 surface area in contact with the liquid helium in the surface magnetic field region alone, and the power density is 1.2×10^{-4} watts/cm^2.

Therefore the reentrant cavity can be cooled by contact with liquid helium at any temperature, but the split ring (and to a lesser extent the helix) requires a forced flow (which raises the temperature and thus the surface resistance) or superfluid helium refrigeration, which will put it off the optimum operating temperature.

3.4 *Electronics*

The two features which a booster linac for a tandem must have are the variable velocity profile and the high energy resolution which impose fairly stringent requirements on the electronics powering and controlling the resonator fields. The variable velocity profile feature requires that every resonator is independent, and its relative phase can be adjusted at will. This in turn means that a complete electronics package must be provided for every resonator to independently power and control it. The high energy resolution imposes requirements on amplitude and phase stability which are orders of magnitude more stringent than that for any operational linacs, thus requiring these control packages to regulate the cavity fields to high precision. In addition, each control package must provide for cavity tuning as well as prevention of electro-mechanical instabilities. Both of these functions are complicated by the extremely narrow bandwidths and sensitivity to noise of superconducting cavities (see Section 2). Because each electronic control package must perform all these fairly complex functions to extremely high precision and because of their great number, the total cost of the accelerator electronics could render the accelerator prohibitively expensive.

However, because of the low rf power requirements of superconducting resonators and the availability of cheap and reliable solid-state rf devices, it is possible to power and control a superconducting resonator at only a small fraction of the total accelerator cost. This is particularly true for the more stable resonators such as the reentrant cavity, which do not use pin diode switched reactive tuners. These frequency tuners,[31] when designed to correct large frequency deviations, must handle relatively high power levels, hundreds of watts to kilowatts. This power is mostly reactive, but its circuit comes out of the cryostat and thus involves loss of normal metal and the cryogenic inconvenience of the power leads. The advantage of such tuners is the large gain-bandwidth product, which is important in stabilizing resonators against electromechanical oscillations.

Figure 8 shows a tentative electronics block diagram for a heavy-ion linac. The control

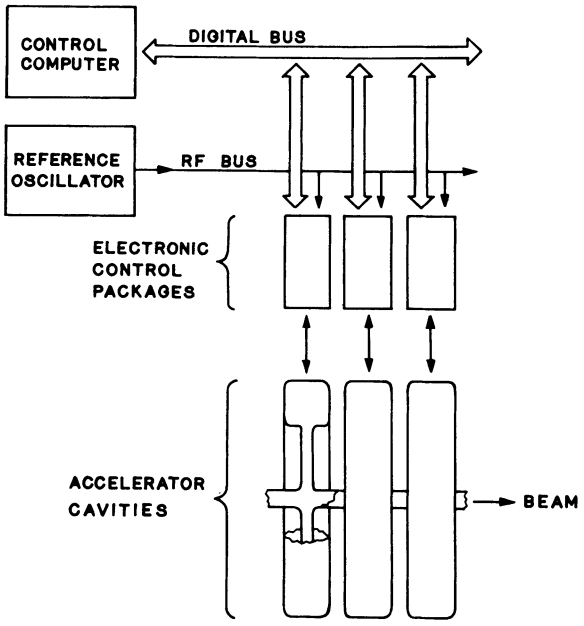

FIGURE 8 Electronics block diagram for an independently phased superconducting reentrant cavity linac.

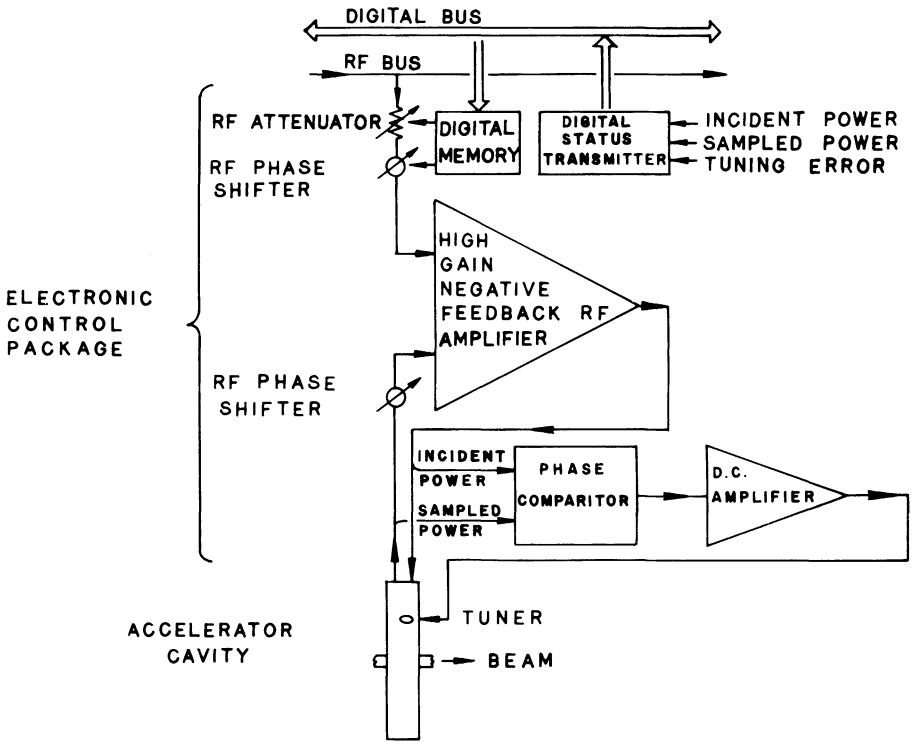

FIGURE 9 Cavity control package block diagram.

computer calculates the amplitude and phases of the fields in the individual cavities necessary to accelerate a certain ion to a given velocity. It then relays this information to the electronic control packages (one per cavity) which in turn regulates the fields to the prescribed values. A reference oscillator and distribution bus provide the individual electronic packages with a phase and amplitude reference. In addition to initially setting the phases and amplitudes values in the electronic control packages, the computer can monitor their performance through the digital bus to detect any malfunctioning.

A block diagram of an exemplary electronic package is shown in Figure 9. The phase and amplitude values provided by the control computer are stored in a digital memory. This digital information is used to control an electronic rf attenuator and phase shifter which in turn modify the rf reference signal entering the control package to the values prescribed by the computer. A high-gain rf amplifier, operating in a negative feedback mode, compares this modified rf reference signal with an rf signal sampled from the cavity fields and works to minimize any difference by applying the proper rf power to the cavity. Thus, the rf amplifier forces the cavity fields to match the modified reference signal, both in amplitude and phase. A phase comparator measures the phase difference between the incident and sampled rf signals and produces a tuning error signal which in turn drives a cavity tuner. The status transmitter converts certain important information, such as cavity input power, sampled power and tuning error into digital form at the control computer's command and so allows the computer to monitor the performance of the electronic control package and cavity and check for malfunctioning.

Except for the digital control and the direct rf feedback, the electronic control package is quite typical of that used in many accelerators. In principle, one would not need any feedback, if one were able to apply stable rf power to perfectly tuned cavities. However, since tuners are usually mechanical devices and quite slow, they are not normally able to keep the cavities perfectly tuned in the presence of vibrations of the cavity walls. Because of such limitations, one normally uses a feedback system that electronically controls the incident rf power, both in amplitude and phase and so stabilized the cavity rf amplitude and phase in

spite of any tuning error. In this case, the tuner is only required to keep the cavity's resonant frequency to within several bandwidths of the accelerator frequency to allow the rf amplifier to drive the cavities.

An alternative electronics package design is described in Ref. 20. This package uses phase and amplitude detectors and dc amplifiers instead of the direct rf feedback. It performed well in beam tests of reentrant cavities. The package provides all the necessary control functions for a cavity, and fits into a triple module NIM plug-in unit.

4 RESONATOR CONSTRUCTION AND PROCESSING

The most complex subject in the construction of a superconducting ion linac is the making of a successful superconducting resonator.

Preparing an operational resonator involved a number of steps, which can be divided into two main categories: a) Construction, involving steps like forming, machining and welding; b) Processing, involving mechanical, chemical and electrical polishing, cleaning, anodyzing and ultra high vacuum (UHV) firing. For practical reasons some of the processing steps have to fall inbetween construction steps.

The general techniques used in the construction and processing of any resonator are the same, but there are differences in detail and procedure. Therefore, in the following sections, whenever the discussion has to go into details which are resonator dependent, the reentrant cavity will be used.

Reentrant cavities have been studied in a research collaboration of Stanford University and the Weizmann Institute of Science for the past six years in an effort to develop the technology of superconducting heavy-ion linac.

Some of the techniques used in making the reentrant cavities were borrowed from L-band cavity procedures developed for the superconducting electron linac at Stanford. A few improvements have been made, some of which made possible by the particular shape of the reentrant cavities.

4.1 Choice of Material

The niobium stock used was supplied by Wah Chang Co., Albany, Oregon. Purity specifications are given in Table I. The niobium was supplied as rolled plates, 19 × 19 × 0.2 in., which are later cut into circular plates.

The niobium is required to be dense, and free of voids, and have grain size no larger than ASTM No. 5. The last requirement is related to the subsequent forming operation, which also requires the niobium to be fully annealed and 95% recrystallized. We have experimented with a cavity with large grain size, constituted of about six single crystals a few inches long, and found no significant difference from small-grain cavities.

4.2 Forming

The simple shape of reentrant cavities makes it possible to use inexpensive manufacturing techniques, suitable for mass production. The cavities were made in two halves, each cavity hydroformed in a single stroke to nearly its final shape.

In hydroforming a single die is used and a flexible membrane forces the niobium plate to conform with the die shape by hydrostatic pressure. This process is not very accurate although its accuracy can be improved by stress relief and an additional hydroforming, or by making allowances for springback in the die design. It is also possible to improve accuracy by resorting to a two-die press forming. In our case the inaccuracies were removed by machining.

A separate step was taken to form the connection to the beam tube in the center, and to rf coupling holes on the circumference. As explained in Ref. 1 there is a certain advantage in performing these welds as far as possible from high-field regions. This was done by extruding the niobium, pulling it as far as possible outwards at these spots. This extrusion was done by drilling a small hole in the center of the spot, placing a specially formed die on one side, a punch on the other and exerting pressure on the punch. The punch penetrates the hole and pulls the metal around until it is stopped by the die.

The extrusion of the rf window is done after the half cavity has been machined, since its existence interferes with turning the shell on the lathe.

4.3 Machining

Each half cavity is turned on a lathe and the contour is traced by following a template. Rough cuts are made no more than 0.02 in., and final cuts between 0.002 to 0.01 in. Turning speeds of around 300 rpm and feeds of around 0.005 in. are typical. Cooling

is done with spray mist, e.g., DoAll's Klean Kool. Rapid Tap can give a better surface finish, but is difficult to use because of the hazardous fumes it produces. High-speed tools should be used, and it is very important to have a sharp tool. Machining properties of niobium are similar to soft copper, but it is abrasive and wears down tools, and it is "gummy," tends to stick and tear which makes it imperative to use sharp tools, and has a positive rake of about 5–10°. Roughing tool could be similar to Kennametal VNMS 331-K68, and final cut tool was made of Unimet TPG-221-U-20 on which a sharp edge is ground to cut and remove the niobium drips.

4.4 *Electron Beam Molten Zone Welds*

The molten zone welding technique was developed to assemble niobium cavities by electron beam welding. The interior surfaces of the cavity are not easily accessible after assembly, chemical processing is done before welding, so that the welding technique must leave them clean and smooth.

The joint region for the molten zone welding takes up about one-half of the wall thickness. The inner side from the joint through the rest of the wall thickness opens up in the form of a V of about 30°.

To secure 100% penetration of the weld without permitting the electron beam to enter the cavity, the beam is defocused releasing its energy at the surface of the weld and creating a pool of molten metal deep enough to reach the interior of the joint.

The purpose of the V interior to the weld is to focus surface tension forces by curving the interior surface of the molten metal, thus preventing the spattering of small drops which frequently occurs when electron beam welding niobium. The welding parameters are not very critical. Spatter-free welds can be obtained with the configuration described, a welding speed of 15 in. per minute, a beam defocused to $\frac{1}{16}$ in. diameter circle, a beam voltage of 100 kV and a beam current of 20 mA. On varying beam voltage or current, spatter appears at a voltage of 120 kV or a current of 28 mA. The focus is the most sensitive setting as it is not always a uniform disc, being a function of gun filament and alignment configurations. Before embarking on a welding job, therefore, it is prudent to check the beam properties on a test piece.

4.5 *Annealing and Stress Relieving*

The niobium has to be annealed before the hydroforming. To prevent spring back of the hydroformed sections they have to be stress relieved before machining. It is advisable to weld the struts (see later) to the cavity before this step, so that strains created by the weld will be relieved. It was found that welding creates severe stress, which may show up after machining, therefore the procedure should be: annealed niobium is hydroformed, some machining is done to fit the struts, the struts are welded, then the assembly is stress relieved, and then it is machined. After machining the sections should be annealed again, since it was found that chemical polishing and electro-polishing works better on annealed niobium. After the chemical treatment comes the final weld, and then the assembled structure is UHV fired. UHV firing will be discussed in more detail later. Adequate stress relieving is done at 1150°C for 3 hours at vacuum near 10^{-6} Torr. Annealing can be done at 1200°C to 1400°C.

4.6 *Struts*

The strength of niobium is severely reduced at elevated temperatures; therefore, to prevent dimensional changes during high-temperature firing we found it necessary to weld six struts to each side of the cavity. These struts are made of the alloy Cb10W, which is niobium with 10% tungsten (and a small quantity of zirconium). This alloy's thermal expansion coefficient is not significantly different from pure niobium, but has a much higher yield strength at elevated temperatures.

In addition to high-temperature strength, the struts increase the rigidity of the cavity by orders of magnitude at lower temperatures if they are also welded to the next cavity, to form an I beam shape which resists bending modes. The advantage here is in making this relatively stable heavy-ion accelerating structure even more stable.

4.7 *Processing Techniques*

A "good" cavity, i.e., a cavity capable of a high Q and high fields, must be clean and smooth. The objective of this section is to describe how to produce good reentrant cavities.

One cannot overemphasize the demand for clean operating conditions. Degreasing the niobium thoroughly prior to chemical operation, using reagent grade chemicals, wearing gloves, dust free rooms, thorough rinses, all these precautions should be regarded. In addition, exposure of the clean surface to air should be minimized or avoided after firing and especially after initial operation. On top

of that, the layer of niobium which is damaged or work hardened by machining has to be removed, and the finished cavity must be pumped to ultra high vacuum (UHV) before operation.

The following subsections describe processing methods which have been used successfully on reentrant cavities. These methods aim at achieving a clean bare niobium surface. Another method was developed at the Karlsruhe Nuclear Research Center and Siemens AG Research Laboratories. This method is based on a surface treatment only, without UHV firing, and the final inner surface of the resonator is anodized. This method is not suitable for reentrant cavities which are sensitive to multipactoring, since an anodized cavity is highly susceptible to multipactoring.

4.8 Chemical Polishing

This operation was used on a number of reentrant cavities, and in conjunction with UHV firing gets good results.

The chemical polishing solution consists of 60% HNO_3 (conc.) and 40% HF (60%) held at 0°C. The cavity is polished with constant agitation for a period of about 4 minutes which removes about 25 μm of the surface. Besides removing work-hardened material, this process also gives a smooth surface. However, extended chemical polishing etches single crystal grains differentially, thus producing a sharp boundary, which is further enhanced by the increased activity of the solution in grain boundaries. To minimize the time necessary to remove tool marks, which extend into the niobium surface as work-hardened regions, we polished the cavity mechanically using, in the final stages, fine alumina powder (600 grit) as an abrasive. Machining damage extends to about 25 μm below the surface so that it is recommended to remove altogether a little over 25 μm. 50 μm should be enough for the worst case. However, removal of a large layer, 100 μm or more, produces etching of the surface and sharp grain boundaries, and should be avoided. For a cavity which has no deep machine-hardened surface very little chemical polishing is needed (e.g., a cavity that has been chemically cleaned before but became contaminated). For slow chemical cleaning, the acid should be precooled to -10°C. If the cavity is large, it should also be precooled. At this temperature the niobium is removed at a rate of 1–2 μ/minute.

It is extremely important to rinse the cavity in distilled water immediately after polishing. A small quantity of acid on the niobium surface will heat up in a very short time due to the chemical activity, and will etch the surface.

Rinsing is repeated until litmus paper indicates that all acid has been rinsed away. The final rinse is done with technical grade metanol to remove the water.

4.9 Electropolishing

Electropolishing offers some distinct advantages over chemical polishing, and should be used whenever the geometry of the cavity permits. The main advantages are improved surface furnish which gives higher Q values and higher field performance, the possibility of removing considerable thickness off the surface without etching, no differential etching of single crystal grains of different orientation or grain boundaries, and lesser dependence on local disturbance of the solution flow.

The best method of electropolishing niobium was developed at Siemens Research Laboratories.[32] The electrolyte used is 95–97% sulphuric acid and 40% hydrofluoric acid in a ratio of 81 : 10 by volume. A high purity aluminum electrode is used, with geometry conforming to the niobium anode. The chemicals should be reagent grade, and the temperature controlled to a constant value between 25°C and 30°C. The mean current density is of the order of 100 mA/cm^2, and the voltage is between 9 and 15 volts and should be well regulated. The operating point in voltage is determined by the onset of current oscillations, which start with a modulation of about 50% and dies in about 2 to 3 minutes. Once the oscillations stop the voltage should be switched off, and the solution stirred for about 4 minutes. During this time the oxide buildup is dissolved by the solution and the process can repeat. Since one cycle removes slightly under 1 μm, a large number of cycles is necessary, and the process should be automated. However, changes in the various parameters, such as solution concentration, change the operating point, so that some supervision must be maintained.

One additional problem is the formation of hydrogen bubbles, which should not be allowed to stick to the niobium surface. For this reason, and also for the convenient insertion of an electrode, we electropolish the niobium cavities while they are in two halves, and keep the electropolished surface facing upwards.

4.10 *Anodization*

Anodic oxide films on niobium surfaces are used mainly for three purposes:

1) Protective coating between intermediate preparation steps.
2) Controlled removal of very thin surface layers.
3) Supply of oxygen during intitial stage of UHV firing.

An example for the first application is anodyzation immediately following chemical polishing or electropolishing, and before the major electron beam weld is done. In this example the oxide layer provides protection of the clean surface from atmospheric contamination, the relatively poor vacuum (which includes oil vapor) of the electron beam welder, and possible microscopic niobium dust or droplets produced by the welding process. After welding, and prior to UHV firing, the oxide layer, together with the contaminations, is removed by 25% HF, and then the cavity is anodized once more.

An example for the second application is treatment of an assembled cavity which has been exposed to contamination after the UHV firing. The cavity is anodized and then the oxide is removed by HF. A repeated sequence of anodization-stripping is referred to as oxipolishing and can improve the surface finish. However, this is a slow process and should not be considered as a substitute to electropolishing.

The purpose of the third application is to get rid of an excess of carbon in the niobium by providing a controlled quantity of oxygen to the surface of the cavity during UHV firing. The evidence for improved results is not conclusive.

There are various anodizing solutions such as dilute nitric acid, dilute sodium hydroxide, dilute sulfuric acid at room temperature, or 1% phosphoric acid at 65°C. The solution which is most often used is room temperature 25% ammonia. The main advantage of this solution is its degreasing properties. It is very convenient to use and can produce thick films. To avoid forming crystalline oxide, which can be removed only by mechanical polishing, the maximum voltage should be kept below 100 V (equivalent to about 0.2 μm oxide layer), and current density should be maintained between 3 to 5 mA/cm^2. This method produces the desired amorphous Nb_2O_5.

4.11 *UHV Firing*

The ultra high vacuum firing is the last treatment the cavity gets before assembly in the cryostat. The firing temperature found to give the best results for the reentrant cavities is about 1800°C. The time to reach the high temperature is a function of the outgassing rate and the pumping capacity. At the high temperature 10 hours seem to give sufficient results. It is desirable to cool the cavity as fast as possible down to room temperature.

The vacuum system should be as clean as possible. It is impossible to measure the vacuum at the hot zone near the cavity (or preferably inside the cavity), and experimental figures are given for the vacuum far from the hot zone. The UHV firing system which is used in the reentrant cavities processing sequence at Stanford employs a dual vacuum system, where the inner volume of the cavities being fired is pumped separately from the exterior. The vacuum on the exterior is the furnace vacuum, and it is on the order of 10^{-8} Torr during the run, and approaches 10^{-9} Torr after cool-down. This vacuum is obtained with a 220 L/S ion pump in combination with a titanium sublimation pump housed in a water-cooled chamber of about 16 in. diameter. The furnace insulation is of the multifoil type[33] and the power consumption is about 12 KW at 1800°C for a hot zone 16 in. diameter by 12 in. long.

The cavity vacuum is measured outside the furnace, and therefore the measurement does not represent the true pressure in the cavity. However, the vacuum at that point reached about 10^{-10} Torr after cooldown. The vacuum in the cavity during the run is limited by diffusion through the 0.5 cm thick walls, but a gradient of about an order of magnitude in pressure is expected, so that one gains by this double vacuum system method.

However, the most significant advantage of this furnace is the possibility to close the valves on each side of the accelerating structure without ever letting gas into the cavities. Keeping the cavities evacuated after the UHV firing up to and including assembly in the accelerator and beam tests, improves the results in peak field, residual surface resistance and consistency of the performance.[34,35]

4.12 *Helium-Ion Processing*

This processing technique[13] is important on a few accounts. It is simple, and involves no extra equipment other than what one normally has in the

accelerator. It gives a considerable improvement in performance, and what is most significant, it is done on the accelerator structure while it is installed on the beam line and cooled down. The principle is very simple: a low pressure, clean helium gas is admitted into the cavities, which are operated at the highest possible field. The helium atoms are ionized by electron streams which come out of field emission sites and accelerated by the electromagnetic field towards the field emission site. Thus any "bad spot" in the cavity is bombarded by helium ions, and gets cleaned, meaning that the field emission loading is reduced by orders of magnitude.

The drawback of this processing method is that one has to begin with a relatively good cavity. Otherwise either the field levels are too low for efficient helium ion bombardment, or the surface resistance deteriorates. It has been observed that cavities which are UHV fired and then tested without being exposed to air (Section 4.11.) are particularly good candidates to helium-ion processing. In the reentrant cavities which were processed in this way no deterioration was observed in the surface resistance, while the field emission limit was pushed up to nearly 22 MV/m in a few instances.[35]

The helium-ion processing will be a major maintenance method in cryogenic accelerators, and used to clean up cavities which have been lightly contaminated.

ACKNOWLEDGEMENTS

It is a pleasure to acknowledge the hospitality of Stanford University, where the experimental work was done, and in particular the support and interest of Profs. H. A. Schwettman and S. S. Hanna.

The author wishes to acknowledge with thanks the contribution made to the work by his former colleague P. H. Ceperley, and the critical reading of the manuscript by J. S. Sokolowski.

REFERENCES

1. I. Ben-Zvi, P. H. Ceperley, and H. A. Schwettman, *Particle Accelerators*, **7**, 125 (1976).
2. J. S. Sokolowski, P. H. Ceperley, M. Samuel, M. Birk, H. F. Glavish, and S. S. Hanna, *IEEE Trans. Nucl. Sci.*, **NS-24**, 1141 (1977).
3. J. L. Fricke, B. Piosczyk, J. E. Vetter, and H. Klein, *Particle Accelerators*, **3**, 35 (1972).
4. J. E. Vetter, G. Hochschild, B. Piosczyk, E. Jaeschke, R. Repnow, and Th. Walcher, Proceedings of the 1976 Proton Linear Accelerator Conference, Chalk River, AECL 5677, p. 106.
5. K. W. Shepard, J. E. Mercereau, and G. J. Dick, *IEEE Trans. Nucl. Sci.*, **NS-22**, 1179 (1975).
6. L. M. Bollinger, R. Benaroya, B. E. Clift, A. H. Jaffey, K. W. Johnson, T. K. Khoe, C. H. Scheibelhut, K. W. Shepard, and T. P. Wangler, Proceedings of the 1976 Proton Linear Accelerator Conference, Chalk River, AECL 5677, p. 95
7. J. P. Turneaure, Proc. 8th Int. Conf. on High Energy Accelerators, CERN, 1972, p. 51.
8. J. Halbritter, *Z. Physik*, **266**, 209 (1974).
9. P. H. Ceperley, High Energy Physics Laboratory Report No. 655, Stanford University, 1971.
10. B. Hillenbrand, H. Martens, K. Schnitzke and H. Diepers, Proc. 9th Int. Conf. on High Energy Accelerators, Stanford, 1974, p. 143.
11. B. Hillenbrand, H. Martens, H. Pfister, K. Schnitzke, and Y. Uzel, *IEEE Trans. Magn.*, **MAG-13**, 491 (1977); P. Kneisel, H. Kupfer, W. Schwarz, O. Stoltz, and J. Halbritter, *IEEE Trans. Magn.*, **MAG-13**, 496; G. Arnolds and D. Proch, *IEEE Trans. Magn.*, **MAG-13**, 500.
12. K. Agyeman, I. M. Puffer, J. A. Yasaitis, and R. M. Rose, *IEEE Trans. Magn.*, **MAG-13**, 343 (1977).
13. H. A. Schwettman, J. P. Turneaure, and R. F. Waites, *J. Appl. Phys.*, **45**, 914 (1974).
14. J. Halbritter, Interner Bericht 73-20-LIN, Kernforschungszentrum Karlsruhe, 1973.
15. J. Halbritter, Externer Bericht 3/72-3, Kernforschungszentrum Karlsruhe, 1972.
16. J. P. Turneaure, Proc. of 1972 Applied Superconductivity Conference, *IEEE* 72CH0682-S-TABSC, 621 (1972).
17. K. Mittag, *Cryogenics*, **13**, 94 (1973).
18. G. J. Dick and G. D. Sprouse, *IEEE* **MAG-13**, No. 1, 512 (1977).
19. H. Klein, P. Junior, J. Klabunde, O. Siart, H. Deitinghoff, P. Finke, and A. Schempp, *Proc. of the Int. Conf. on Nuclear Reactions Induced by Heavy Ions* (North-Holland Publishing Co., Heidelberg, 1970) p. 540.
20. P. H. Ceperley, H. F. Glavish, S. S. Hanna, M. Samuel, and J. S. Sokolowski, *IEEE* **MAG-13**, No. 1, 520 (1976).
21. A. Branderlik, A. Citron, P. Flecher, J. L. Fricke, R. Hietschold, G. Hochschild, G. Hornung, H. Klein, G. Krafft, W. Kuhn, M. Kuntze, B. Piosczyk, E. Sauter, A. Schempff, D. Schulze, L. Szecsi, J. E. Vetter, and K. W. Zieher, *Particle Accelerators*, **4**, 111 (1972).
22. J. S. Sokolowski, private communication.
23. I. Ben-Zvi, *Particle Accelerators*, **7**, 125 (1977).
24. Z. Segalov and I. Ben-Zvi, Proc. 2nd Int. Conf. on Electrostatic Accelerators, Strassburg, 1977.
25. L. M. Bollinger, T. K. Khoe, F. J. Lynch, B. Zeidman, R. Benaroya, J. J. Bicek, Jr., B. E. Clifft, A. H. Jaffey, K. W. Johnson, J. M. Nixon, and W. A. Wesolowski, *IEEE Trans. Nucl. Sci.*, **NS-22**, 1148 (1975).
26. This cryostat was constructed by Ricor Ltd., Ein Harod, Israel.
27. I. Ben-Zvi, B. Elkonin and N. Pundak, to be submitted to Cryogenics.
28. L. R. Suelzle, *IEEE Trans. Nucl. Sci.*, **NS-18**, 146 (1971).
29. M. S. McAshan, H. A. Schwettman, L. Suelzle, and J. P. Turneaure, High Energy Physics Laboratory Report No. 665, Stanford University, 1972.
30. T. R. Strobridge, *IEEE Trans. Nucl. Sci.*, **NS-16**, 1104 (1969).
31. G. Hochschild, D. Schulze, and F. Spielbock, *IEEE Trans. Nucl. Sci.*, **NS-20**, 116 (1973).

32. H. Diepers, O. Schmidt, H. Martens, and F. S. Sun, *Phys. Lett.*, **37A**, 139 (1971).
33. M. L. Paquin, Multi Foil Thermal Insulation, Thermo Electron Corporation, Waltham, Mass. (1972).
34. P. H. Ceperley, I. Ben-Zvi, H. F. Glavish, and S. S. Hanna, *IEEE Trans. Nucl. Sci.*, **NS-22**, 1153 (1975).
35. P. H. Ceperley, J. Sokolowski, I. Ben-Zvi, H. F. Glavish, and S. S. Hanna, *Nucl. Inst. Methods*, **136**, 421 (1976).